Draft version January 12, 2016
Preprint typeset using LaTeX style emulateapj v. 04/17/13

# EFFECT OF BEAM CHROMATICITY ON FOREGROUNDS IN WIDE-FIELD MEASUREMENTS OF REDSHIFTED 21 CM POWER SPECTRA

Nithyanandan Thyagarajan[1*], TBD

*Draft version January 12, 2016*

## ABSTRACT

*Keywords:* cosmology: observations — dark ages, reionization, first stars — large-scale structure of universe — methods: statistical — radio continuum: galaxies — techniques: interferometric

## 1. INTRODUCTION

The period in the history of the Universe characterized by the transition of neutral hydrogen in the intergalactic medium (IGM) to a fully ionized state due to the formation of radiating objects such as the first stars and galaxies is referred to as the Epoch of Reionization (EoR). This is an important period of nonlinear growth of matter density perturbations and astrophysical evolution leading to the large scale structure observed currently in the Universe. And yet, this period in the Universe's history has remained poorly probed to date with observations.

The redshifted neutral hydrogen from the IGM in this epoch has been identified to be one of the most promising and direct probes of the EoR (Sunyaev & Zeldovich 1972; Scott & Rees 1990; Madau et al. 1997; Tozzi et al. 2000; Iliev et al. 2002). Numerous experiments using low frequency radio telescopes targeting the redshifted 21 cm line from the spin-flip transition of HI have become operational such as the Murchison Widefield Array (MWA; Lonsdale et al. 2009; Bowman et al. 2013; Tingay et al. 2013), the Precision Array for Probing the Epoch of Reionization (PAPER; Parsons et al. 2010), the Low Frequency Array (LOFAR; van Haarlem et al. 2013) and the Giant Metrewave Radio Telescope EoR experiment (GMRT; Paciga et al. 2013). These instruments have sufficient sensitivity for a statistical detection of the EoR signal via estimating the spatial power spectrum of the redshifted HI temperature fluctuations (Beardsley et al. 2013; Thyagarajan et al. 2013). These instruments are intended to be precursors and pathfinders to the next generation of low frequency radio observatories such as the Hydrogen Epoch of Reionization Array[3] (HERA; DeBoer et al. 2015) and the Square Kilometre Array[4] (SKA). These next-generation instruments will advance the capability from a mere statistical detection of the signal to a direct three-dimensional tomographic imaging of the HI during the EoR.

The most significant challenge to low frequency EoR observations arises from the extremely bright Galactic and extragalactic foreground synchrotron emission which are $\sim 10^4$ times stronger than the desired EoR signal (Di Matteo et al. 2002; Ali et al. 2008; Bernardi et al. 2009, 2010; Ghosh et al. 2012). All the current and future instruments rely on the inherent differences in spatial isotropy and spectral smoothness between the EoR signal and the foregrounds to extract the EoR power spectrum (see, e.g., Furlanetto & Briggs 2004; Morales & Hewitt 2004; Zaldarriaga et al. 2004; Santos et al. 2005; Furlanetto et al. 2006; McQuinn et al. 2006; Morales et al. 2006; Wang et al. 2006; Gleser et al. 2008).

When expressed in the coordinate system of power spectrum measurements described by the three-dimensional wavenumber ($k$), the foreground emission is restricted to a wedge-shaped region commonly referred to as the *foreground wedge* (Bowman et al. 2009; Liu et al. 2009, 2014a,b; Datta et al. 2010; Liu & Tegmark 2011; Ghosh et al. 2012; Morales et al. 2012; Parsons et al. 2012; Trott et al. 2012; Vedantham et al. 2012; Dillon et al. 2013; Pober et al. 2013; Thyagarajan et al. 2013; Dillon et al. 2014) whereas the EoR signal has spherical symmetry due to its isotropy which appears elongated along line of sight $k$ modes due to peculiar velocity effects when dominated by matter density perturbations during early stages of reionization. The extreme dynamic range required to subtract foregrounds precisely demands high precision modeling of foregrounds as observed by modern wide-field instruments (Thyagarajan et al. 2015b,a).

## 2. THE HYDROGEN EPOCH OF REIONIZATION ARRAY

DeBoer et al.(2016)

## 3. DELAY SPECTRUM

(Parsons et al. 2012)

### 3.1. *The Wide-Field "Pitchfork" Effect*

(Thyagarajan et al. 2015b,a)

## 4. SIMULATIONS

We simulate wide-field visibilities for 19-element HERA from all-sky antenna power pattern and foreground models using the PRISim[5] software package. The simulations cover 24 hr of observation in *drift* mode consisting of 80 accumulations spanning 1080 s each. The total bandwidth is 100 MHz centered on 150 MHz consisting of 128 channels with 781.125 kHz frequency resolution each. Models of the antenna power pattern and foregrounds are described below.

### 4.1. *Antenna Power Pattern*

(Neben et al. 2015)

[1] Arizona State University, School of Earth and Space Exploration, Tempe, AZ 85287, USA
[*] e-mail: t_nithyanandan@asu.edu
[3] http://reionization.org/
[4] https://www.skatelescope.org/

[5] The Precision Radio Interferometry Simulator (PRISim) is publicly available at https://github.com/nithyanandan/PRISim

### 4.2. *Foreground Model*

Our all-sky foreground model is the same as the one in Thyagarajan et al. (2015b). It consists of diffuse emission (de Oliveira-Costa et al. 2008) and point sources. The latter is obtained from a combination of the NRAO VLA Sky Survey (NVSS; Condon et al. 1998) at 1.4 GHz and the Sydney University Molonglo Sky Survey (SUMSS; Bock et al. 1999; Mauch et al. 2003) at 843 MHz with a mean spectral index of -0.83. The diffuse sky model has an angular resolution of 13.′74.

## 5. CHROMATICITY OF POWER PATTERN

The equation for delay spectrum describes the mapping between sky location of a foreground object and delay. The chromatic nature (variation with frequency) of the antenna power pattern results in a convolution of the geometrical mapping with the delay response of spectral chromaticity of the power pattern. This can result in a significant spillover of foreground power beyond the horizon delay limits especially in the case of foregrounds near the horizon.

Fig. 1 demonstrates the beyond-the-horizon spillover even from a flat-spectrum point source at different off-axis angles. The three panels correspond to delay spectra from different positions of the point source – 0°(left), 45°(middle) and 89°(right) – from the zenith. The phase centers are located at the source positions and hence the delay spectra are centered on $\tau = 0$ ns. The response of the simulated dish power pattern (dashed line) is comapred with that from an *Airy* pattern resulting from a nominal uniformly illuminated circular disk (solid line). The gray vertical lines correspond to the horizon limits at $\pm 48.7$ ns for a 14.6 m antenna spacing.

At 0°off-axis, the *Airy* pattern has no spectral variation and thus appears as a straight vertical line centered at $\tau = 0$ ns whereas the simulated power pattern is found to exhibit some spectral variation giving rise to the wings on either side of $\tau = 0$ ns. As off-axis angle increases to 45°, both the power patterns clearly exhibit chromaticity. They have similar magnitudes inside the horizon limits but the chromaticity of the simulated power pattern is $\sim 100$ times higher than that of an *Airy* pattern outside the horizon limits. In contrast, at 89°off-axis, the two patterns have similar chromaticity in delay modes outside the horizon limits but the simulated power pattern has $\sim 100$ times more power inside the horizon limits indicating that the overall amplitude of the pattern at this location is higher relative to the nominal *Airy* pattern.

It is important to note that in a generic scenario where visibilities are not phased to a specific foreground location, the chromaticity of the power pattern will imprint itself on location of the foreground objects in delay space and will give rise to significant spillover especially from foregrounds near the horizon.

We investigate the effects of spectral chromaticity of the power pattern in more detail below.

### 5.1. *Directional Chromaticity*

### 5.2. *Effect on Delay Power Spectrum*

### 5.3. *Constraints on Antenna-to-Antenna Reflections*

Patra et al. 2015 (submitted), Ewall-Wice et al. 2015 (submitted)

## 6. SUMMARY

This work was supported by the U. S. National Science Foundation (NSF) through award AST-1109257. DCJ is supported by an NSF Astronomy and Astrophysics Postdoctoral Fellowship under award AST-1401708. JCP is supported by an NSF Astronomy and Astrophysics Fellowship under award AST-1302774.

## REFERENCES

Ali, S. S., Bharadwaj, S., & Chengalur, J. N. 2008, MNRAS, 385, 2166
Beardsley, A. P., Hazelton, B. J., Morales, M. F., et al. 2013, MNRAS, 429, L5
Bernardi, G., de Bruyn, A. G., Brentjens, M. A., et al. 2009, A&A, 500, 965
Bernardi, G., de Bruyn, A. G., Harker, G., et al. 2010, A&A, 522, A67
Bock, D. C.-J., Large, M. I., & Sadler, E. M. 1999, AJ, 117, 1578
Bowman, J. D., Morales, M. F., & Hewitt, J. N. 2009, ApJ, 695, 183
Bowman, J. D., Cairns, I., Kaplan, D. L., et al. 2013, PASA, 30, 31
Condon, J. J., Cotton, W. D., Greisen, E. W., et al. 1998, AJ, 115, 1693
Datta, A., Bowman, J. D., & Carilli, C. L. 2010, ApJ, 724, 526
de Oliveira-Costa, A., Tegmark, M., Gaensler, B. M., et al. 2008, MNRAS, 388, 247
Di Matteo, T., Perna, R., Abel, T., & Rees, M. J. 2002, ApJ, 564, 576
Dillon, J. S., Liu, A., & Tegmark, M. 2013, Phys. Rev. D, 87, 043005
Dillon, J. S., Liu, A., Williams, C. L., et al. 2014, Phys. Rev. D, 89, 023002
Furlanetto, S. R., & Briggs, F. H. 2004, New A Rev., 48, 1039
Furlanetto, S. R., Oh, S. P., & Briggs, F. H. 2006, Phys. Rep., 433, 181
Ghosh, A., Prasad, J., Bharadwaj, S., Ali, S. S., & Chengalur, J. N. 2012, MNRAS, 426, 3295
Gleser, L., Nusser, A., & Benson, A. J. 2008, MNRAS, 391, 383
Iliev, I. T., Shapiro, P. R., Ferrara, A., & Martel, H. 2002, ApJ, 572, L123
Liu, A., Parsons, A. R., & Trott, C. M. 2014a, Phys. Rev. D, 90, 023018
—. 2014b, Phys. Rev. D, 90, 023019
Liu, A., & Tegmark, M. 2011, Phys. Rev. D, 83, 103006
Liu, A., Tegmark, M., Bowman, J., Hewitt, J., & Zaldarriaga, M. 2009, MNRAS, 398, 401
Lonsdale, C. J., Cappallo, R. J., Morales, M. F., et al. 2009, IEEE Proceedings, 97, 1497
Madau, P., Meiksin, A., & Rees, M. J. 1997, ApJ, 475, 429
Mauch, T., Murphy, T., Buttery, H. J., et al. 2003, MNRAS, 342, 1117
McQuinn, M., Zahn, O., Zaldarriaga, M., Hernquist, L., & Furlanetto, S. R. 2006, ApJ, 653, 815
Morales, M. F., Bowman, J. D., & Hewitt, J. N. 2006, ApJ, 648, 767
Morales, M. F., Hazelton, B., Sullivan, I., & Beardsley, A. 2012, ApJ, 752, 137
Morales, M. F., & Hewitt, J. 2004, ApJ, 615, 7
Neben, A. R., Bradley, R. F., Hewitt, J. N., et al. 2015, ArXiv e-prints, arXiv:1505.07114
Paciga, G., Albert, J. G., Bandura, K., et al. 2013, MNRAS, 433, 639
Parsons, A. R., Pober, J. C., Aguirre, J. E., et al. 2012, ApJ, 756, 165
Parsons, A. R., Backer, D. C., Foster, G. S., et al. 2010, AJ, 139, 1468
Pober, J. C., Parsons, A. R., Aguirre, J. E., et al. 2013, ApJ, 768, L36
Santos, M. G., Cooray, A., & Knox, L. 2005, ApJ, 625, 575
Scott, D., & Rees, M. J. 1990, MNRAS, 247, 510
Sunyaev, R. A., & Zeldovich, Y. B. 1972, A&A, 20, 189

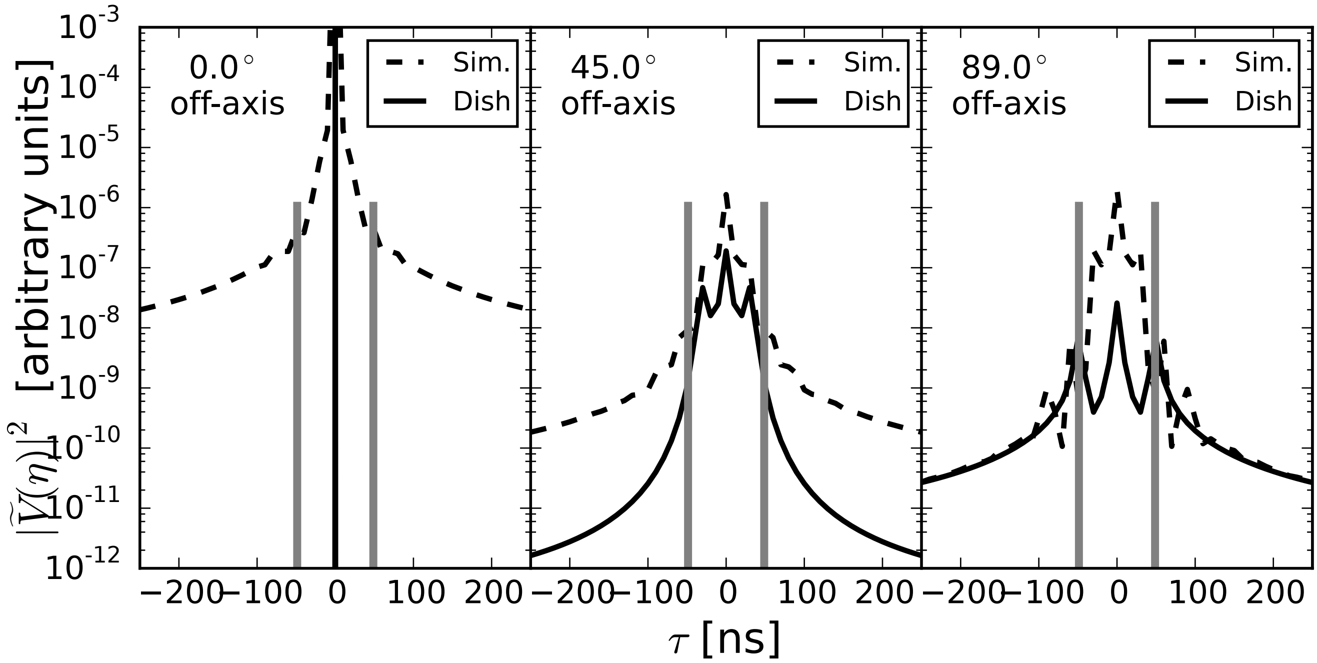


**Figure 1.** Chromaticity of antenna power pattern at directions off-axis.

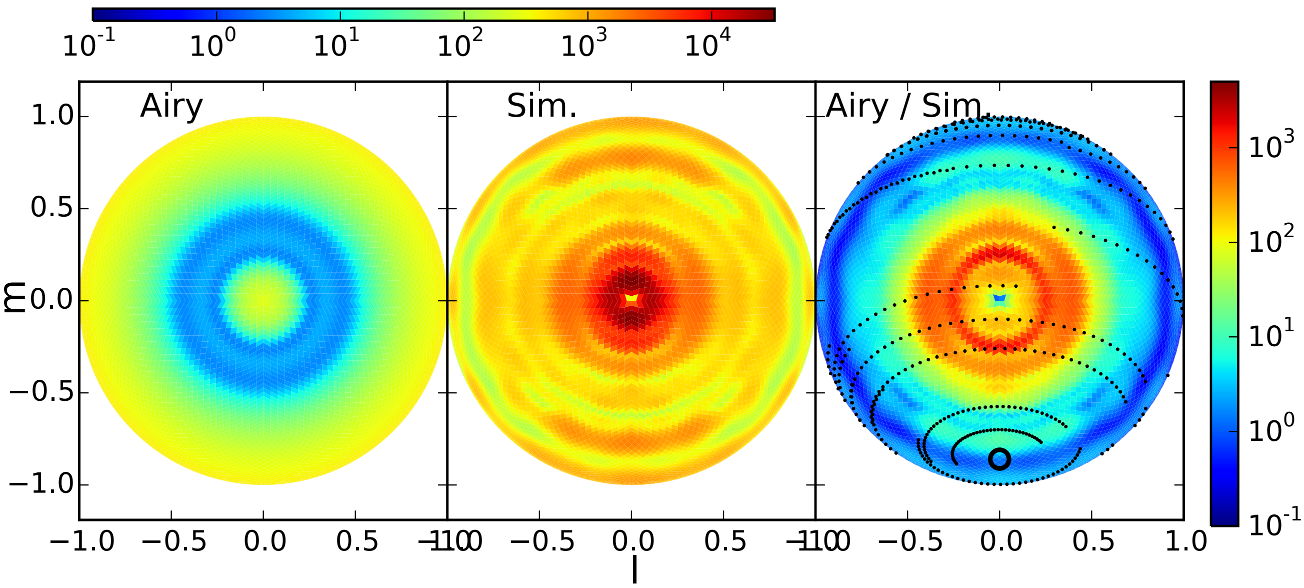


**Figure 2.** All-sky directional chromaticity of antenna power pattern.


Thyagarajan, N., Udaya Shankar, N., Subrahmanyan, R., et al. 2013, ApJ, 776, 6
Thyagarajan, N., Jacobs, D. C., Bowman, J. D., et al. 2015a, ApJ, 807, L28
—. 2015b, ApJ, 804, 14
Tingay, S. J., Goeke, R., Bowman, J. D., et al. 2013, PASA, 30, 7
Tozzi, P., Madau, P., Meiksin, A., & Rees, M. J. 2000, ApJ, 528, 597
Trott, C. M., Wayth, R. B., & Tingay, S. J. 2012, ApJ, 757, 101
van Haarlem, M. P., Wise, M. W., Gunst, A. W., et al. 2013, A&A, 556, A2
Vedantham, H., Udaya Shankar, N., & Subrahmanyan, R. 2012, ApJ, 745, 176
Wang, X., Tegmark, M., Santos, M. G., & Knox, L. 2006, ApJ, 650, 529
Zaldarriaga, M., Furlanetto, S. R., & Hernquist, L. 2004, ApJ, 608, 622

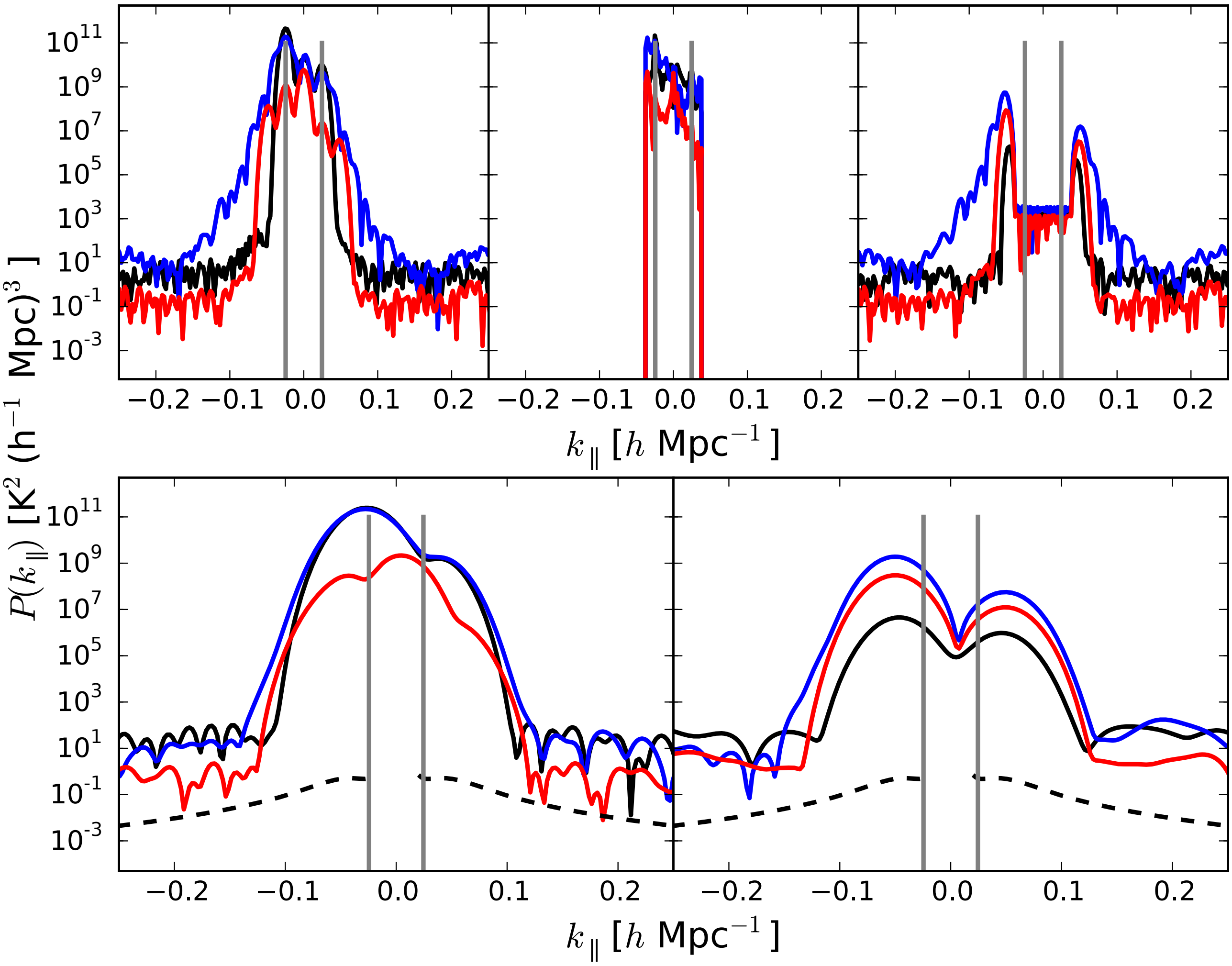


**Figure 3.** Effect of chromaticity of antenna power pattern on foreground delay power spectra.

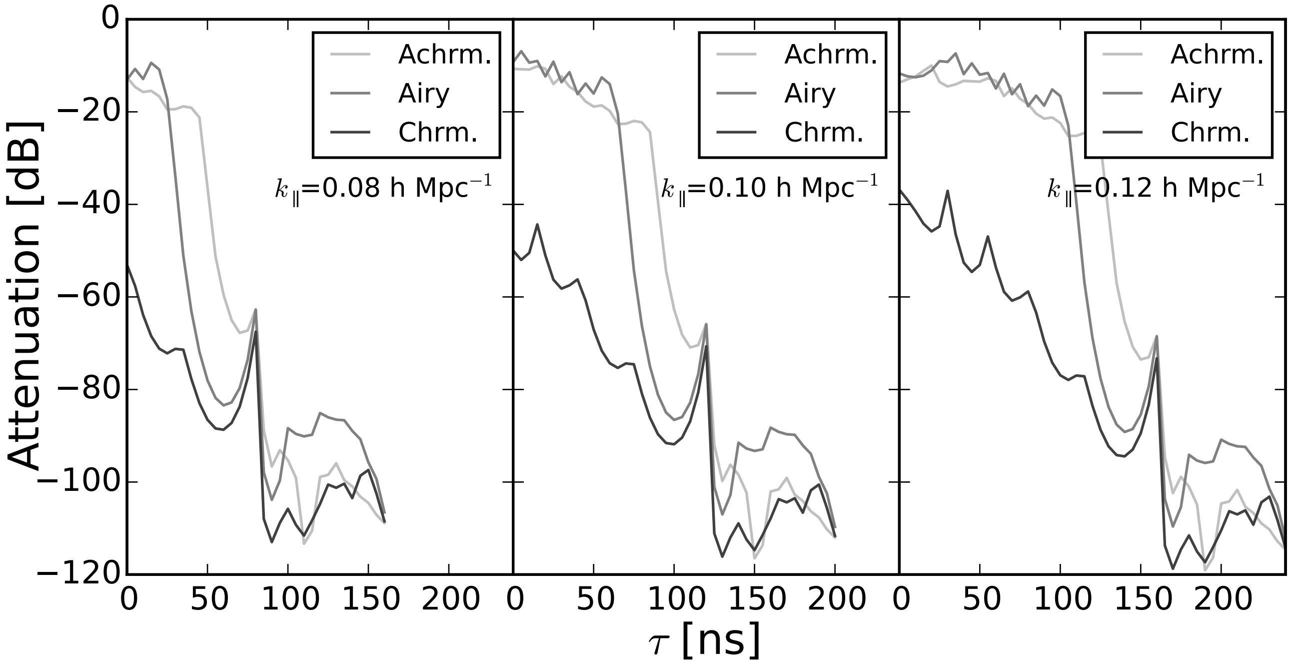


**Figure 4.** Attenuation of foreground power (in dB) from antenna-to-antenna reflections required to keep the reflected foreground power below EoR HI signal power.